BOND BEHAVIOUR OF NSM CFRP-CONCRETE SYSTEMS: ADHESIVE AND CFRP CROSS-SECTION INFLUENCES

J. Cruz [1], A. Borojevic [1], J. Sena-Cruz [1], E. Pereira [1], P. Fernandes [1], P. Silva [1] and A. Kwiecien [2]

[1] ISISE, School of Engineering, University of Minho, Portugal. Email: jsena@civil.uminho.pt

[2] Department of Civil Engineering, The Cracow University of Technology, Poland.

ABSTRACT

Near Surface Mounted (NSM) strengthening technique has been used in a sustainable way for retrofitting existing structures. This technique, which utilizes CFRP laminates inserted in the concrete cover, has been used due to the several advantages when compared with the technique based on the application of these reinforcing materials on the concrete surface (EBR technique). Although several studies have been developed on this topic in the recent past, open issues still deserve research, such as the influence of the adhesive type on the performance of the NSM-CFRP system. The present work details an experimental program carried out in order to assess the effect of using three adhesives with distinct mechanical properties on the bond behavior of the NSM-CFRP system, through direct pullout tests (DPT). Thus, the following variables were considered in the present study: (i) the type of adhesive; (ii) the cross-section of the laminate; and, (iii) the bond length. The experimental pullout force-slip responses were obtained and digital image correlation (DIC) was used for obtaining additional information about the bond mechanisms developed. In general, two of the three adhesives, with similar mechanical characteristics, provided essentially similar bond behavior, with high level of effectiveness, whereas the third adhesive, which had a much lower elastic modulus than the other two, provided the lowest effectiveness in terms of the investigated parameters.

KEYWORDS

NSM, CFRP, Direct Pullout Test, bond, adhesive.

INTRODUCTION

Fibre reinforced polymers (FRP) have been extensively investigated for repairing and/or strengthening existing structures. These materials can be introduced in the concrete cover of the element to be strengthened through the near surface mounted (NSM) technique. An epoxy adhesive is commonly used to fix the CFRP laminate to concrete. This bonding agent plays a critical role on the composite performance of the system. Extensive research has been developed to assess the bond behaviour of this strengthening system using carbon fibre reinforced polymers (NSM CFRP system). According to Coelho *et al.* (2015) the performance of the NSM CFRP system depends mainly on the: (i) geometry of the groove and of the FRP; (ii) mechanical properties of the concrete; (iii) mechanical properties of the adhesive; (iv) FRP cross-section and its external surface; and, (v) surface roughness in the groove. Digital Image Correlation (DIC) is a method that allows to evaluate the displacement fields at the surface of a structural element, as well as to compute the deformation fields during the test. Essentially the method is based on comparing two consecutive images of the element surface, before and after its deformation, through the application of an appropriate correlation technique (Chu *et al*. 1985). More information about this technique can be found elsewhere (e.g., Pereira *et al.* 2012; Carloni and Subramaniam 2013). In the literature few investigations can be found dedicated to analyzing the influence of adhesive and cross-section geometry of the laminate on the bond behavior of NSM CFRP system, e.g. Macedo *et al.* (2008).

In this research the effect of three adhesives for fixing CFRP laminates to concrete substrate according to the NSM technique is analyzed, by means of direct pullout tests. The main motivation for testing two stiff adhesives and one of much lower stiffness lies on the reported advantage of using highly deformable (flexible) adhesives in external bonding (EB) of CFRP laminates to RC beams as strengthening (Derkowski et al. 2013). In this research the type geometry of the CFRP cross-section as well as the bond length were also analyzed and as study variables. The experimental program is detailed and the main results are presented and analyzed in the subsequent sections.

EXPERIMENTAL PROGRAM

Test program, specimens and test configuration

The experimental program was composed of 51 direct pullout tests (DPT) where the influence of adhesive type, cross-section geometry and bond length of the bond NSM CFRP system were analysed. Table 1 presents the experimental program which includes: (i) three adhesive types - Adhesive 1 (ADH1), 2 (ADH2) and 3 (ADH3); (ii) two cross-sections of CFRP laminate - 10×1.4 mm^2 (L10) and 20×1.4 mm^2 (L20); and, (iii) six bond lengths (L_b) - 50, 60, 80, 100, 200 and 300 mm. Concrete cubic specimens were adopted with L_b values up to 100 mm, while concrete prismatic specimens were adopted with L_b values of 200 and 300 mm. Each series was composed of 3 specimens, being its generic denomination ADH**X**_L**YY**_Lb**ZZ**, where X represents the adhesive type (1, 2 or 3), YY is the width of CFRP in millimeters and ZZ indicates the bond length also in millimeters.

Table 1 Experimental program.

Type of adhesive	Type of specimen's geometry	CFRP cross-section geometry, $w_f \times t_f$ [mm^2]	Bond length [mm]	Series
Adhesive 1 (ADH1)	Cubic	10×1.4 (L10)	60	ADH1_L10_Lb60
			80	ADH1_L10_Lb80
			100	ADH1_L10_Lb100
	Cubic	20×1.4 (L20)	80	ADH1_L20_Lb80
			100	ADH1_L20_Lb100
	Prismatic		200	ADH1_L20_Lb200
			300	ADH1_L20_Lb300
Adhesive 2 (ADH2)	Cubic	20×1.4 (L20)	80	ADH2_L20_Lb80
			100	ADH2_L20_Lb100
	Prismatic		200	ADH2_L20_Lb200
			300	ADH2_L20_Lb300
Adhesive 3 (ADH3)	Cubic	10×1.4 (L10)	50	ADH3_L10_Lb50
			100	ADH3_L10_Lb100
			150	ADH3_L10_Lb150
	Cubic	20×1.4 (L20)	80	ADH3_L20_Lb80
			100	ADH3_L20_Lb100
	Prismatic		300	ADH3_L20_Lb300

The geometry of the pullout specimens and test configuration adopted for both types of geometries is presented in Figure 1. In the cubic specimen, which consisted on concrete cube blocks with 200 mm of edge, grooves were performed on their lateral faces with a cross-section geometry of 5×15 mm^2 in general, or 5×25 mm^2 for insertion of CFRP laminates L10 and L20, respectively. In order to avoid the premature specimen failure by the formation of a concrete fracture cone between the load end and the top of the block, 100 mm of unbounded zone was guaranteed between these two points (in the case of ADH3 series the distance adopted was 50 mm). A steel plate of 20 mm of thickness was used to fix the upper part of the concrete block to the stiff base through four M10 steel threaded rods, ensuring negligible vertical displacements. In the prismatic specimens, which consisted of concrete prisms of $150\times150\times600$ mm^3, only grooves with a cross-section of 5×25 mm^2 for insertion of laminates L20 were performed. The distance between the loaded end and the top of the prism was also equal 100 mm. The specimen was supported on a steel frame through a steel plate, threaded rods, horizontal bars and a hydraulic jack. The tests were performed under displacement control at the loaded end adopting two displacement rates: for stiff adhesives ADH1 and ADH2, 2 µm/s, and for flexible adhesive ADH3, 5 µm/s. A load cell, placed between the grip and the actuator, was used to measure the applied force, F, and a linear variable displacement transducer - LVDT1 - was used to measure the loaded end slip (relative displacement between the concrete and the CFRP laminate at the loaded end).

In order to help with interpreting the evolution of the degradation mechanisms of the anchorage zone during testing, the surface of the specimens at which the laminates were inserted was analysed using a Digital Image Correlation procedure (Blaber *et al.*, 2015). The evolution of the crack pattern was documented during the monotonic loading by processing a sequence of images with a constant time step. The lens used had an aperture of f11 and the focal length was 100 mm. Led lights were used to illuminate the surface of the specimen. The camera sensor was a full frame size, with 36 Mpix. Considering that the priority was to trace the initiation and propagation of the cracks during testing, the principal tensile strain fields were mapped considering a very fine facet mesh. This mapping was particularly important to identify the location of the first cracks with respect to the CFRP laminate load end and to document the process of initiation and propagation of new cracks during the entire loading sequence.

Materials characterization

The compressive strength of the concrete was assessed using cylinders with 150 mm of diameter and 300 mm of height, at 28 and 110 days after casting. The modulus of elasticity and the compressive strength were assessed according to LNEC E-397-1993:1993 and NP EN 12390-3:2009 recommendations, respectively. An average modulus of elasticity (E_{cm}) of 27.0 GPa, with a coefficient of variation, CoV, of 0.5% and an average compressive strength (f_{cm}) of 35.4 MPa (CoV = 4.8 %) were obtained at 28 days. At 110 days, E_{cm} = 28.3 GPa (CoV = 2.5%) and f_{cm} = 38.5 MPa (CoV = 2.1%) were obtained. The mechanical properties of the adhesives were assessed according to ISO 527-2:2012. The following average values were obtained for the elastic modulus (E_a) and tensile strength (f_a): ADH1 - E_a=11.67 GPa (CoV = 0.51%) and f_a=25.59 MPa (CoV = 7.40%); (ii) ADH2 - E_a=7.57 GPa (CoV = 6.15%) and f_a=17.19 MPa (CoV = 5.43%); (iii) ADH3 - E_a=0.012 GPa (CoV = 9.09%) and f_a=2.67 MPa (CoV = 12.49%). The mechanical properties of CFRP laminates can be found in (Fernandes *et al.* 2015) for L10 and in (Sena-Cruz *et al.* 2013) for L20.
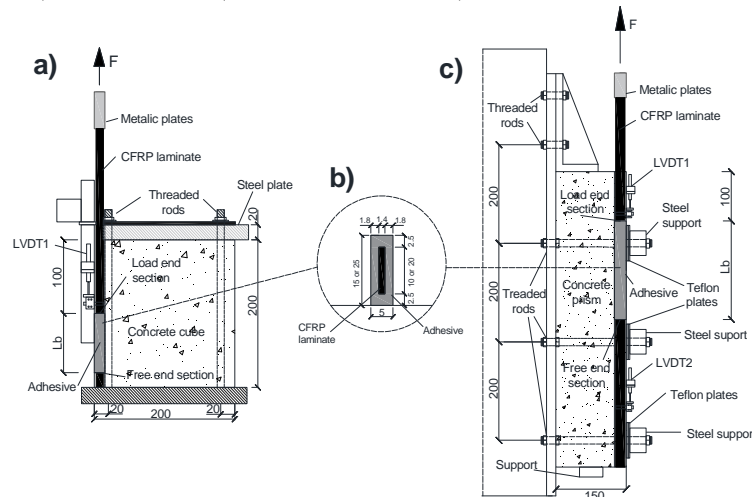

Figure 1 Geometry of specimens and test configuration: (a) cubic concrete specimen (axial cross-section); (b) groove detailing; (c) prismatic concrete specimen (axial cross-section).

RESULTS AND DISCUSSIONS

Main results

Table 2 presents the main results obtained from the pullout tests, including the average results for each series, as well as the observed failure modes, including: F_{lmax} is the maximum pullout force reached during the test; $\tau_{max,avg}$ is the average shear bond strength at laminate-adhesive interface, which was computed by dividing F_{lmax} by the contact area between the CFRP laminate and the adhesive, $2 (w_f + t_f) L_b$, (see Fig. 1b, where w_f and t_f are the width and the thickness of the CFRP laminate, respectively and L_b represents the bond length); s_{lmax} is the slip at F_{lmax}. Typical average pullout force *versus* loaded end slip ($F_l – s_l$) relationships are presented in Figure 2. The responses are similar to those obtained by e.g. Fernandes *et al.* (2015). They are mostly non-linear, probably as a result of the non-linear behaviour of the adhesive, as well as due to the debonding process. For the series ADH1 and ADH2, short post-peak branches are observed, related to the failure mode in the form of debonding at the laminate-stiff adhesive interface. On the other hand, the responses obtained for series ADH3 are characterized by the long post-peak branches, related to cohesive failure in the flexible adhesive. Comparing the response of series ADH1 and ADH2 with the response of ADH3, significantly higher ultimate loads F_{lmax} are obtained for the stiff adhesives and significantly higher slip s_l for the flexible adhesive. Simultaneously, ADH3 provides lower stiffness on the NSM CFRP system than ADH1 and ADH2, but higher ductility.

Failure modes

Failure modes obtained in ADH1 and ADH2 series include the debonding at the laminate-adhesive interface (see Figure 3(a) – microscope photography) and laminate failure (see Figure 3(b)). In series ADH3 the failure mode observed was a mixed failure mode, i.e., specimens failed due to debonding at laminate-adhesive interface in some parts of the bond length, as well as due to the cohesive failure of the adhesive close to laminate-adhesive interface on the other parts (see Figure 3(c)).

Table 2 Main results obtained from the pullout tests.

Type of adhesive	Type of laminate	Series	F_{lmax} [kN]	$\tau_{max,avg}$ [MPa]	s_{lmax} [mm]	F_{lmax}/f_{fu} [%]	FM
ADH1	L10	ADH1_L10_Lb60	22.49 (1.5%)	16.44 (1.5%)	0.50 (13.8%)	60.77 (1.5%)	I-FA(3)
		ADH1_L10_Lb80	25.97 (2.1%)	14.24 (2.1%)	0.68 (3.3%)	70.20 (2.1%)	I-FA(3)
		ADH1_L10_Lb100	29.57 (3.4%)	12.97 (3.4%)	0.93 (7.1%)	79.92 (3.4%)	I-FA(3)
	L20	ADH1_L20_Lb80	46.69 (4.5%)	13.63 (4.5%)	0.50 (7.0%)	58.36 (4.5%)	I-FA(2)
		ADH1_L20_Lb100	48.91 (4.1%)	11.43 (4.1%)	0.64 (7.1%)	61.14 (4.1%)	I-FA(3)
		ADH1_L20_Lb200	59.53 (3.0%)	6.95 (3.0%)	1.10 (22.7%)	74.41 (3.0%)	I-FA(1);F(1)
		ADH1_L20_Lb300	61.03 (2.6%)	4.75 (2.6%)	1.27 (17.2%)	76.28 (2.6%)	F(2)
ADH2	L10	ADH2_L10_Lb60 [1]	24.25 (1.59%)	17.73 (1.59%)	0.55 (11.35%)	65.55 (1.59%)	I-FA(3)
		ADH2_L10_Lb80 [1]	36.52 (2.09%)	20.02 (2.09%)	0.88 (2.15%)	98.71 (2.09%)	F(3)
		ADH2_L10_Lb100 [1]	35.60 (2.98%)	15.61 (2.98%)	0.81 (10.98%)	96.22 (2.98%)	F(3)
	L20	ADH2_L20_Lb80	48.40 (4.6%)	14.13 (4.6%)	0.48 (29.0%)	60.50 (4.6%)	I-FA(3)
		ADH2_L20_Lb100	54.06 (4.4%)	12.63 (4.4%)	0.75 (11.9%)	67.57 (4.4%)	I-FA(3)
		ADH2_L20_Lb200	55.19 (6.4%)	6.45 (6.4%)	0.88 (10.0%)	68.98 (6.4%)	I-FA(1);F(1)
		ADH2_L20_Lb300	60.36 (3.4%)	4.70 (3.4%)	2.01 (17.7%)	75.45 (3.4%)	I-FA(2);F(1)
ADH3	L10	ADH3_L10_Lb50	2.35 (6.0%)	2.06 (6.0%)	1.12 (11.2%)	6.34 (6.0%)	I-FA+C-A(3)
		ADH3_L10_Lb100	5.03 (6.9%)	2.21 (6.9%)	1.33 (14.7%)	13.59 (6.9%)	I-FA+C-A(3)
		ADH3_L10_Lb150	8.12 (6.3%)	2.38 (6.3%)	1.71 (2.9%)	21.95 (6.3%)	I-FA+C-A(3)
	L20	ADH3_L20_Lb80	5.71 (11.8%)	1.67 (11.8%)	1.88 (7.4%)	7.14 (11.8%)	I-FA+C-A(3)
		ADH3_L20_Lb100	9.89 (0.5%)	2.31 (0.5%)	2.11 (4.0%)	12.36 (0.5%)	I-FA+C-A(2)
		ADH3_L20_Lb300	28.57 (10.4%)	2.22 (10.4%)	2.71 (20.6%)	35.71 (10.4%)	I-FA+C-A(3)

Notes: the values between parentheses are the corresponding coefficients of variation (CoV); FM (Failure Modes): I-FA = Debonding failure at laminate-adhesive interface; C-A = Cohesive failure of adhesive close to laminate-adhesive interface; F = CFRP failure; the values between parentheses are the number of specimens where this failure occurred. [1]Results collected from publication Sena-Cruz *et al.* (2015).
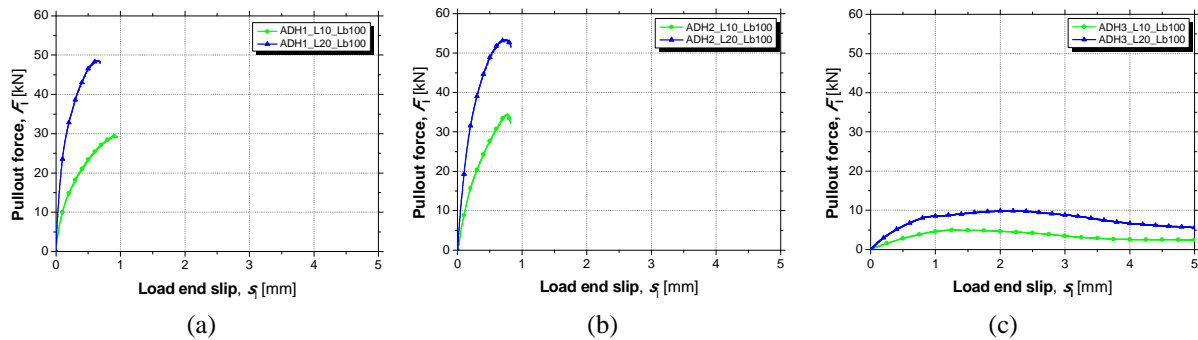

(a)   (b)   (c)

Figure 2 Typical average pullout force *vs.* loaded end slip relationship, obtained in the experimental program for the same bond length of L_b= 100 mm and two CFRP width: (a) ADH1; (b) ADH2; (c) ADH3.
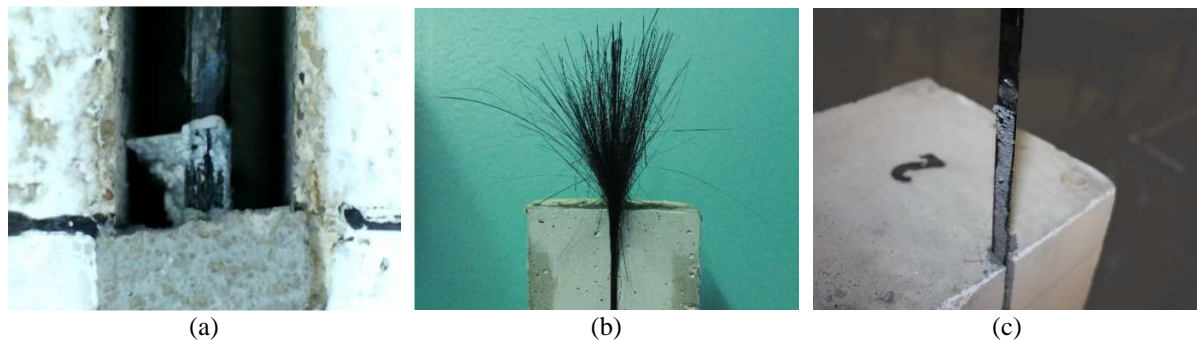

(a)   (b)   (c)

Figure 3 Failure modes observed in the experimental program: (a) and (b) ADH1 and ADH2; (c) ADH3.

Influence of study variables on the bond behaviour

The influence of adhesive type and cross-section geometry of the CFRP laminate were assessed for different bond lengths, and the summary of the results is presented in Figure 4. As expected, and in accordance to the literature (e.g. Sena-Cruz 2005; Coelho *et al.* 2015; Peng *et al.* 2015), F_{lmax} tends to increase with the increase of L_b, coinciding the upper limit of F_{lmax} with the tensile strength of the CFRP laminate (e.g. ADH2_L10 series with L_b of 80 and 100 mm). F_{lmax} is higher for L20 series than L10 series, which probably is related to the higher contact area at both interfaces and the consequent superior capacity of stress transfer from the laminate to

concrete. In general according to F_{lmax}, less stiff ADH2 is more efficient than stiffer ADH1, while ADH3 provides F_{lmax} values significantly lower than the previous ones. For instance, in series L20 for_Lb80 the F_{lmax} obtained with ADH3 is only 12% of the average value obtained when ADH1 and ADH2 are used. However, the performance of ADH3 tends to be closer to series ADH1 and ADH2 with the increase of L_b (see series L20 with_Lb300).

$\tau_{max,avg}$ tends to decrease with the increase of L_b for ADH1 and ADH2 (stiffer adhesives) due to the higher contact area between the CFRP and adhesive and the non-uniform distribution of bond stresses along the bond length, as referred and justified in (Coelho *et al.* 2015). Using ADH3 (flexible adhesive), it can be noted that $\tau_{max,avg}$ tends to be similar for all tested bond lengths, which can be justified by a better and more uniform distribution of bond stresses along L_b, due to the lower stiffness of the adhesive ADH3, which has an elasticity modulus three orders of magnitude lower than the ones of ADH1 and ADH2. The cross-section geometry of the laminate did not significantly influence $\tau_{max,avg}$, in the present work: $\tau_{max,avg}$ was fond to be similar for L10 and L20, for the tested bond lengths (except ADH2 series). This finding probably demonstrates that the bond stress development at laminate-adhesive interface is independent of the cross-section of the laminate. Finally, it can be noted that the adhesive type has a significant influence on $\tau_{max,avg}$. Series ADH2_L10 reached higher $\tau_{max,avg}$ values than series ADH1_L10, while on ADH1_L20 and ADH2_L20 the values obtained were similar in both cases. $\tau_{max,avg}$ on series ADH3 was significantly lower than in the case of both ADH1 and ADH2 series.

s_{lmax} also tends to increase with the increase of L_b (except between series ADH2_L10_Lb80 and ADH2_L10_Lb100, probably due to the laminate failure that took place for L_b equal or higher than 80 mm). s_{lmax} is also influenced by the cross-section geometry of the laminate. For instance, for L_b of 80 and 100 mm with ADH1 and ADH2, s_{lmax} tends to be higher for series L10, on contrary to ADH3 where it was higher for laminate L20, namely for L_b of 100 mm. Finally, s_{lmax} is higher for ADH3_L20_Lb300 series than for ADH1_L20_Lb300 and ADH2_L20_Lb300 series.

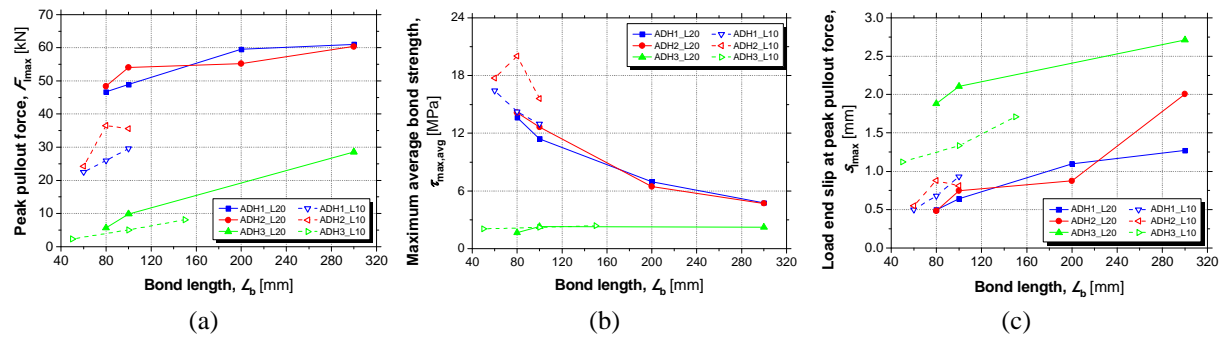
(a)   (b)   (c)

Figure 4 Influence of study variables on the (a) peak pullout force, (b) maximum average bond strength and (c) loaded end slip at maximum pullout force.

Digital Image Correlation Analysis

Figure 5 presents two typical cases where DIC method was applied in order to compare the field strains of stiff and flexible adhesives. Figure 5(a) and Figure 5(b) present the results obtained for specimen ADH1_L20_Lb100_1 ("_1" means the first on specimen of the series) and ADH3_L20_Lb100_1, respectively at peak pullout force. In the first case, diagonal concrete cracks appear, which are caused by the stress transfer from the laminate to the concrete and produces the typical "fish spine" crack pattern due to the resistant mechanisms developed by the system (Sena-Cruz 2005). The use of stiff adhesives tends to lead to the concentration of damage on the concrete surrounding the reinforcing region and at the adhesive-concrete interface, remaining the adhesive almost intact. In contrast, the use of flexible adhesives leads to the significant damage concentration at the adhesive only, remaining the other materials almost intact.

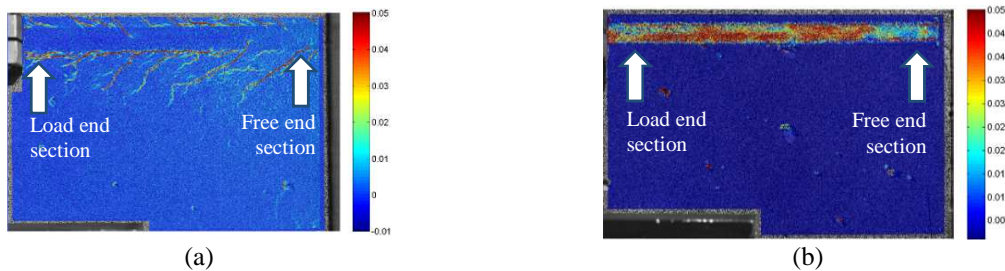(a)   (b)

Figure 5 DIC results obtained for the specimens (principal tensile strains at peak pullout force): (a) ADH1_L20_Lb100_1 and (b) ADH3_L20_Lb100_1. Note: the strains are presented in absolute value.

CONCLUSIONS

This paper presents an experimental research on the bond behaviour of NSM CFRP system and on the evaluation the influence of the following parameters: (i) bonding agents (adhesives) with different mechanical properties; (ii) CFRP cross-section geometry; and, (iii) bond length. This assessment was performed through direct pullout tests (DPT). Specimens failed either by debonding at laminate-adhesive interface or by laminate failure with stiff adhesives depending on the bond length. In specimens strengthened adopting the flexible adhesive, the failure occurred by debonding at laminate-adhesive interface at some parts of the bond length, together with the cohesive failure of adhesive close to the surface of laminate on the remaining parts. In general an increase of the maximum pullout force with the increase of the bond length observed, as well as the greater system efficiency on transferring stress between the laminate and the concrete substrate when the stiff adhesives were used. As expected, the pullout force was higher when the larger cross-section geometry was adopted for the laminate. Moreover, the deformations reached at the same load levels when flexible adhesives were used were significantly higher than the ones obtained when using the stiff adhesives. In general the average bond strength tended to decrease with the increase of bond length when utilising stiff adhesives, remanding approximately constant when the flexible adhesive was used. The cross-section geometry did not significantly influence the average bond strength. Stiff adhesives provided higher values of the average bond strength than flexible adhesives. DIC method allowed to document the development of the bond mechanisms for both types of adhesives during the entire loading sequence. The use of stiff adhesives led to a failure/damage concentration mostly at the concrete substrate and at the laminate-adhesive interface. In contrast, when the softer adhesive was used the damage/failure was found to be in the adhesive.

REFERENCES

Blaber, J., Adair, B. and Antoniou, A. 2015. Ncorr: Open-Source 2D Digital Image Correlation Matlab Software. *Experimental Mechanics* 55:1105-1122.

Carloni, C., Subramaniam, K.V. (2013). "Investigation of sub-critical fatigue crack growth in FRP/concrete cohesive interface using digital image analysis". *Composites Part B: Engineering* 2013;51:35-43.

Chu, T. C., Ranson, W. F. and Sutton, M. A. (1985). "Applications of digital-image-correlation techniques to experimental mechanics", *Experimental Mechanics,* 25, 232-244.

Coelho, M. R. F., Sena-Cruz, J. M. and Neves, L. A. C. (2015). "A review on the bond behavior of FRP NSM systems in concrete", *Construction and Building Materials,* 93, 1157-1169.

Derkowski, W., Kwiecień, A., Zając, B. (2013). "CFRP strengthening of bent RC elements using stiff and flexible adhesives", *Technical Transactions* 1-B/2013, 37-52.

Fernandes, P. M. G., Silva, P. M. and Sena-Cruz, J. (2015). "Bond and flexural behavior of concrete elements strengthened with NSM CFRP laminate strips under fatigue loading", *Engineering Structures,* 84, 350-361.

Macedo, L., Costa, I. and Barros, J. (2008). "Assessment of the influence of the adhesive properties and geometry of CFRP laminates in the bond behavior", *BE2008 – Betão Estrutural 2008,* Guimarães, Portugal.

Peng, H., Hao, H., Zhang, J., Liu, Y. and Cai, C. S. (2015). "Experimental investigation of the bond behavior of the interface between near-surface-mounted CFRP strips and concrete", *Construction and Building Materials,* 96, 11-19.

Pereira, E. B., Fischer, G. and Barros, J. A. O. (2012). "Direct assessment of tensile stress-crack opening behavior of Strain Hardening Cementitious Composites (SHCC)", *Cement and Concrete Research,* 42, 834-846.

Sena-Cruz, J., Fernandes, P., Silva, P., Benedetti, A., Granja, J. and Azenha, M. (2015). "Bond Durability and Quality Control of NSM-Concrete Systems", *COST Action TU1207, Next Generation Design Guidelines for Composites in Construction,* Lecce, Italy.

Sena-Cruz, J., Jorge, M., Branco, J. M. and Cunha, V. M. C. F. (2013). "Bond between glulam and NSM CFRP laminates", *Construction and Building Materials,* 40, 260-269.